University of West Bohemia
Faculty of Applied Sciences
Department of Cybernetics

MASTER'S THESIS

Modelling and experimental validation of signalling pathways with relevance to homologous mammalian systems

Pilsen, 2015 **Tereza Puchrová**

Prohlášení

Předkládám tímto k posouzení a obhajobě diplomovou práci zpracovanou na závěr studia na Fakultě aplikovaných věd Západočeské univerzity v Plzni.

Prohlašuji, že jsem diplomovou práci vypracovala samostatně a výhradně s použitím odborné literatury a pramenů, jejichž úplný seznam je její součástí.

V Plzni dne 30. srpna 2015 Tereza Puchrová

Declaration

I hereby declare that this master's thesis is completely my own work and that I used only the cited sources.

Acknowledgements

I would like to express my sincere gratitude to my advisor, Dr. Daniel Georgiev, who gave me all his support and forwarded his knowledges while guiding me in this project.

Great thanks belong also to my colleagues for helping with the lab work, especially to Hynek Kasl who was helping with the experiments and the data processing.

Finally, I would like to thank my boyfriend and my family for their love and support.

Anotace

Haploidní buňky pivních kvasinek *Saccharomyces cervisiae* používají ke vzájemné komunikaci speciální proteiny, feromony. Receptor, který rozponává feromony v kvasinkách, patří do dobře známé a popsané skupiny receptorů spřažených s G proteinem, které se vyskytují v savčích buňkách, kde umožňují např. čich, reakci imunitního sytému apod. V této práci je představen mechanismus ladění aktivace takového receptoru a uveden jednoduchý model jeho funkce v kvasinkách. Je ukázano, že aktivaci receptoru je možné dynamicky ladit změnou síly zpětné vazby, která odpovídá míře exprese Sst2 proteinu, který je přirozeným negativním regulátorem G proteinu.

Klíčová slova: syntetická biologie, GPCR, Sst2, Ste2, aktivace receptoru, Saccharomyces cervisiae, deterministický model

Abstract

Haploid cells of budding yeast *Saccharomyces cervisiae* use special proteins, called pheromones, for communication. The receptor that recognizes pheromones in yeast belongs to a well-described family of so called GPCRs (G protein-coupled receptors) that are present in mammalian cells enabling the sense of smell, the immune system response, etc. In this work, a mechanism for tuning of the receptor activation is presented and a simple model of the corresponding system inside the yeast is introduced. It is shown that it is possible to dynamically tune the receptor activation by varying the feedback strength corresponding to expression levels of the Sst2 protein which is a native feedback regulator of the G protein.

Keywords: synthetic biology, GPCR, Sst2, Ste2, receptor activation, Saccharomyces cervisiae, deterministic model, yeast pheromone pathway

Contents

1 Introduction

This work focuses on tuning the activation of a cell sensor that can be found in many eukariotic cells including human cells. The sensor is a receptor that belongs to a family of so called GPCRs (G protein-coupled receptors), which is a well-described family of receptors that enable eg. the sense of smell, the immune system response etc. GPCRs are involved in many diseases and represent potential targets for modern medicinal drugs. As such, a vast body of research is dedicated to their characterisation.

The yeast *Saccharomyces cervisiae* GPCR Ste2 is a part of one of the best-known and investigated signalling pathways in yeast - the yeast pheromone pathway. The pathway enables signal transduction from extracellular to intracellular space. The receptor functions as a sensor that detects particular chemical compound in the cell proximity. After detecting the signal, receptor activates a reaction cascade that transfers the information about the chemical presence into the nucleus, where the process of mating is initiated.

Within this work, function of the Ste2 receptor was quantitatively analysed and described mathematically using a simple reduced ODE model. Subsequently a mechanism for tuning receptor activation to control the receptor response was derived and experimentally validated. This tuning mechanism designed for the yeast Ste2 receptor can be applied to any GPCR as it is conserved among various GPCRs. Hence, this work also demonstrates the application of yeast as a model organism for tuning protocols in mammalian cells.

Yeast as a model organism Budding yeast *Saccharomyces cervisiae* is one of the most well-known and studied unicellular eukaryotic organisms. Its complete genome sequence has been mapped in and it is known that a significant amount of yeast genes have their homologs in mammalian cells. It makes yeast a perfect model organism for understanding human DNA sequences and also particular processes within the human cells.

Similar signalling pathways that exist in human cells can be found in yeast and also many human proteins have their yeast homologs with the same functions. Unlike human cells, yeast cells are relatively easy to cultivate and to be genetically manipulated. It is the reason why yeast is often used as a model organism that enables better understanding of processes that would be much more difficult to

investigate *in vivo* (i.e. in human cells).

2 Biological background

2.1 Signal transduction

As mentioned above, the yeast GPCR Ste2 is part of the yeast pheromone pathway which is a signalling pathway that allows a yeast cell to detect and respond to an extracellular signal. This particular signal is in form of pheromone that is produced by another yeast cell. Binding of the pheromone to the receptor activates the receptor and it further activates a reaction cascade that transforms the information about the pheromone presence into an initiation of mating. Yeast pheromone pathway is also often called the mating pathway since the corresponding gene actuation culminates in the mating of two yeast cells. Yeast mating process and the pathway are described in the following sections.

2.1.1 Yeast mating type

Budding yeast exists in either haploid or diploid state. Haploids are of two mating types MATa and MATα that can mate together to form a diploid cell of type MATa/α. Mating is a process of sexual reproduction when two cells of opposite mating type fuse together and form a single cell. Each haploid possesses one copy of each chromosome and after mating, the diploid cell has two copies of each chromosome. In this way, a yeast cell can regain functions lost as a result of DNA damage - by obtaining a healthy chromosome from the mating partner. Besides mating, yeast in both haploid and diploid state can also reproduce non-sexually by mitosis - one cell divides into two, then the daughter cells divide, etc. Also in case of environmental adversity, a diploid can divide into four haploid spores that minimize their energy consumption increasing the likelihood of survival. In a more acceptable environment spores regenerate and the reproduction process stars again (a process called sporulation).

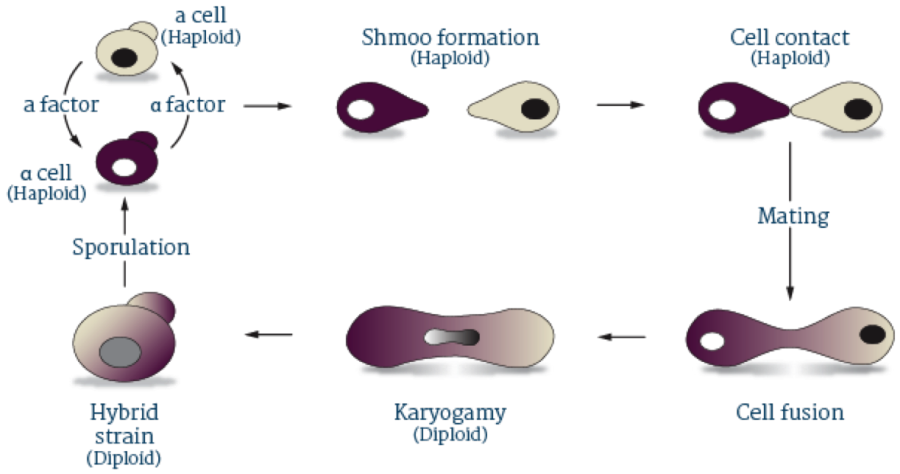

Figure 1: Life cycle of budding yeast. *Source: http://www.renaissanceyeast.com/about/classical-breeding*

In sexual reproduction, haploids use special proteins called pheromones in order to mate efficiently. Both mating types constantly produce small amounts of mating type-specific pheromone and when the two cells of opposite types are in close proximity they identify each other by sensing each other's pheromone. MATa produces pheromone called a-factor and MATα produces α-factor. Yeast cells use GPCRs for detecting pheromones and each mating type has a specific version of this receptor. GPCR of MATa type is the Ste2 protein and that detects α-factor while GPCR of MATα is the Ste3 protein that detects a-factor. After detecting the mating partner's pheromone, activated receptor turns on a cascade of chemical reactions that prepare the cell for the process of mating. It includes expression changes of significant number of genes, cell cycle arrest, and growth toward the mating partner followed by fusion of their membranes. The process of mating takes about 4 h [4].

The whole process of signal transduction from sensing the pheromone to the induction of the mating process is called the yeast pheromone response. The receptor is the only part of the pathway that differs between MATa and MATα, but the functional difference is only in the recognised molecule. The downstream signalling of both GPCRs, Ste2 and Ste3 is identical. Further in this work, the pathway in MATa was investigated.

2.1.2 Yeast pheromone pathway

Yeast pheromone pathway enables cell to respond to a pheromone input by initiating the mating process. The presence of pheromone is an external signal that is processed by the Ste2 receptor. Pheromone activates the receptor and the activated receptor in turn activates a bound G protein that further turns on the mitogen-activated protein kinase (MAPK) cascade. The terminal target of the cascade is Fus3, which transfers high energy phosphate group to specific target molecules. In this case, the specific target is the transcription factor Ste12 that induces synthesis of mating genes in the nucleus.

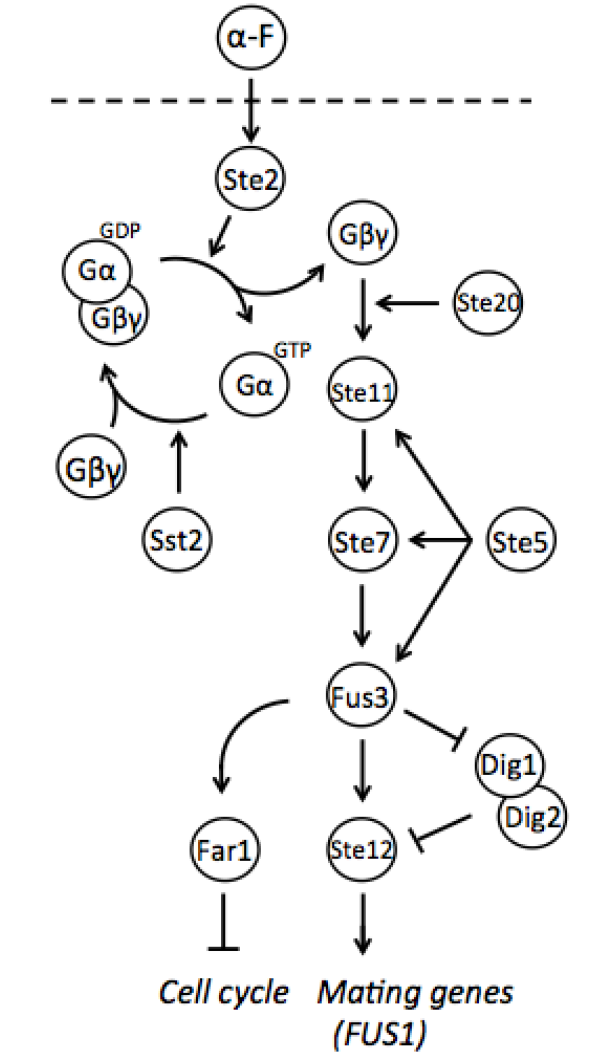

Figure 2: Schematic of the yeast pheromone pathway.

Besides the mating genes induction, also cell cycle is arrested after pheromone exposure. Cell no longer continues its life cycle that consists of repetitive dividing and targets its energy into the process of mating. Observing cell cycle arrest is one of the methods for measuring the pathway response to certain amount of α-factor. This method is described in more detail in the experimental section Sec. 22.

2.2 Highly conserved modules

Yeast pheromone pathway consists of several highly conserved modules that each have functional homologs in human cells. These modules are the Ste2 receptor with the coupled G protein, MAPK cascade, the Ste12 transcription factor, and finally the regulator of G protein signalling (RGS), the Sst2. Protein functions, reaction dynamics, and their regulation is conserved among the species which allows wide use of possible synthetic mechanisms designed in yeast.

GPCR and G protein First module, the Ste2 receptor, is the main part of the pathway. This seven trans-membrane protein is located in cell membrane. Its extracellular part enables binding of α-factor that causes change in the receptor conformation and initiates the activation of coupled G protein that binds the receptor intracellular domain.

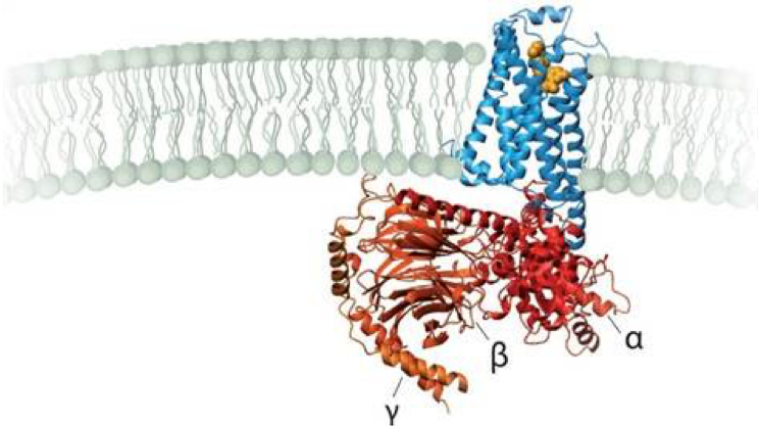

Figure 3: The GPCR structure. *Source: http://imgarcade.com/1/g-protein-coupled-receptors-structure*

G protein consists of three subunits α, β and γ. Gα is bound to Ste2 when the receptor is inactive (in absence of pheromone) and all three subunits are

bound together forming a heterotrimer. In this state, Gα binds GDP and is inactive. After pheromone binding, changed Ste2 conformation causes GDP to GTP exchange on Gα followed by its dissociation and release of the other two subunits. After release, Gβ and Gγ are still bound to each other forming the G$\beta\gamma$ subunit. Gα with bound GTP is in its active state and does not reconstitute with G$\beta\gamma$. G protein is deactivated once GTP on Gα hydrolyses allowing Gα-GDP to re-associates with G$\beta\gamma$.

Unbound active G$\beta\gamma$ initiates the MAPK cascade and the downstream responses so the pathway is only active until Gα-GTP hydrolyses and binds G$\beta\gamma$ again, since G$\beta\gamma$ is active only when apart from Gα. Gα-GTP hydrolysis is induced by Sst2 - the regulator of G protein signalling (RGS). When Sst2 binds Gpa1 (the protein of Gα subunit) it accelerates GTP hydrolysis and thus deactivates the G protein. Gα-GDP then re-associates with G$\beta\gamma$ deactivating the pathway.

GPCRs in eukaryotes are the sensors for diverse extracellular signals and often are linked to MAPK pathways.

MAPK Next module involves a cascade of three kinases where the activation of the first one is induced by the activated G protein (its $\beta\gamma$ subunit), the first activated kinase activates a second one and the second kinase activates a third one - Fus3. The activation happens through phosphorylation which is the forwarding a phosphate group PO_4.

MAPK cascades are frequent key mediators of eukaryotic transcriptional responses to extracellular signals [15]. In many cancer types, it is the defect in MAPK cascade that leads to uncontrolled growth. Therefore parts of MAPK cascade are also targets of a large number of medicinal drugs.

Ste12 Ste12 is a transcription factor that is activated by Fus3 after pheromone exposure. Transcription factors initiate the transcription in response to an extracellular input. They can either block or promote transcription from DNA into RNA and thereby regulate subsequent protein translation. They are found in all organisms where they have the function of gene expression regulators. After being activated via phosphorylation, Ste12 binds DNA regulatory loci that martk the start of mating genes. Binding of the transcription factor enables transcription from the corresponding gene and thus protein production.

Sst2 This regulator protein is the most discussed part in this work and therefore a single section is dedicated to it.

2.3 Activation and regulation of the pathway

Yeast pheromone pathway is activated in presence of a sufficient amount of pheromone. The initiation of mating is a switch-like response. It filters weak pheromone signals to avoid initiation of mating with a partner that is not close enough [10]. Once the pathway is active, the pathway regulators start to deactivate it again so that after mating, the cell can continue its normal life cycle.

One of the pathway regulators was already mentioned, the Sst2, which induces GTPase activity and at the Gα-GTP subunit. Although it is known that Sst2 acts as a negative regulator of G protein activity [2] [3], the precise mechanism of Sst2 action before and after pheromone stimulation is rather unclear.

2.3.1 Sst2, the regulator of G protein signalling

Sst2 is a known regulator of G protein signalling (RGS). RGS proteins strengthen GTPase function of the G protein α-subunits. While receptors stimulate GTP binding resulting in G protein activation, RGS proteins stimulate GTP hydrolysis and thus switch off the signalling pathway activated by the G protein. Sst2 activates GTPase hydrolysing GTP on Gpa1 resulting in de-activation of Gα. Inactive Gα-GDP can then bind G$\beta\gamma$ and block further pathway activation.

The above described Sst2 functions are known and also experimentally validated. Detailed Sst2 behaviour including its effect on the overall pheromone response is not known. There is no uniform opinion on Sst2 changes before and after pheromone exposure. The precise Sst2 turnover after pheromone exposure is also up to debate. Following paragraphs summarise most of the research that has been published regarding Sst2 dynamic behaviour.

Sst2 is expression is induced after pheromone exposure [7]. Sst2 is also phosphorylated in pheromone dependent manner - by active (phosphorylated) Fus3 [6]. Sst2 binds the intracellular tail of Ste2 to localize with its target Gpa1 [3]. When bound to Gpa1 stimulates GTPase activity of Gpa1 resulting in the deactivation of the G protein [2]. It is not clear whether Sst2 phosphorylation has any affect either on Sst2-Gpa1 binding or the GTPase activation.

The rate of Sst2 degradation is also variable but its time dependence is not

consistently reparted in literature. There are three different behaviours presented. Authors of [6] suggest that phosphorylation by Fus3 stabilises the Sst2 protein. This would result in its slower degradation after pheromone exposure. On the other hand, authors of [8] propose that after pheromone exposure, Sst2 is ubiquitinated and then degraded more rapidly. Finally, authors of [16] consider total Sst2 concentration constant for their simulations. Since the opinions on Sst2 dynamics differ, it is difficult to model its behaviour correctly. Nevertheless, clarifying the real mechanism of Sst2 action is crucial for understanding the pathway activation-deactivation mechanism.

Finally, the kinetics of Sst2 have not been studied in detail. First order approximation is commonly used [16]. This work introduces a new insight into Sst2 kinetics, in terms of modelling, supported by mathematical model and experimental results. It is proposed that Gα deactivation by Sst2 has enzymatic kinetics. Thus the hydrolysis rate only depends on concentration of the substrate (Gα-GTP) assuming that total enzyme (Sst2) concentration is constant. Finally, a mechanism for tuning Ste2 receptor activation by Sst2 is introduced.

It has been shown that mutants lacking Sst2 (null mutants) exhibit hypersensitivity to pheromone. Therefore, it seems Sst2 is a critical component of the yeast pheromone pathway preventing hypersensitivity that could cause mis-targeting of the mating partner or the initiation of mating with a partner that is out of reach.

2.4 Dynamics complexity

In biological systems, there are many different nonlinearities that have to be considered and distinguished in the process of modelling. Biochemical reactions are very often nonlinear and their dynamics differ for various types of reactions. Following are the reactions that occur within the pheromone pathway.

- Receptor-ligand binding - the α-factor in the role of ligand binds and activates the Ste2 receptor.
- GDP-GTP exchange - GDP (guanosine diphosphate) exchange for GTP (guanosine triphosphate) on the Gα subunit leading to its activation.
- Phosphorylation - forwarding a phosphate group PO_4. It activates the kinases within MAPK cascade and also the Ste12 transcription factor.

- GTP hydrolysis - dissociation of an inorganic phosphate is promoted by GTPase, a hydrolyse enzyme. It deactivates Gα.
- Transcriptional induction - transcription factors such as Ste12 can promote or repress transcription from a gene by binding or releasing from DNA regulatory parts.

Most of these reactions are included in the models presented. Their structure and dynamics will be described.

3 Modelling and simulations

The purpose of the modelling part of this work was to derive a model useful for tuning of the pheromone pathway activation. The pathway activation depends on the amount of pheromone input. The relationship between the pheromone input and the pathway activation is represented by the dose response curve. Further within this work it is shown how the dose-response curve can be systematically tuned to change the 50% response concentration called the activation threshold (denoted as τ in Fig. 4.

Dose-response curve The dose response curve has a form of a Hill function (see Sec. A for details about Hill function) and it describes an input-output behaviour of the pathway. Input is the amount of α-factor and output is e.g. amount of active Fus3. There are several possible ways of measuring the pathway activation that are related to each other providing the same dose-response curve after normalisation. The methods for measuring dose-response curves is described in Sec. 4.1.

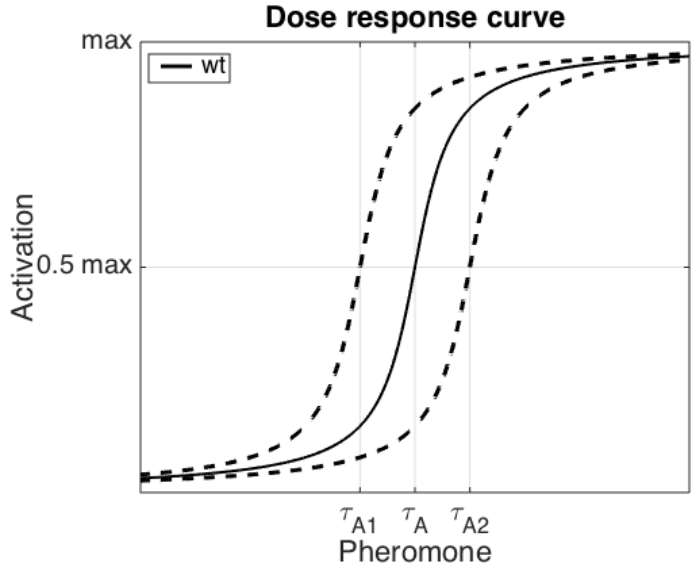

Figure 4: Dose response curve represents a relationship between the amount of input pheromone and the corresponding pathway activation.

Yeast pheromone pathway is a complex system and its complete mathematical model is not intuitive nor easy to understand. Various publications claim to

present complex stochastic [13] or deterministic [9] models of the whole pathway. Others seek to simplify the whole system and focus only on the mechanism of interest while neglecting (or reducing) the rest. Such work is usually context specific focused on some particular part of the pathway.

Herein, a complex stochastic model of the whole yeast pheromone pathway [13] is presented first. This model was used for early testing of hypotheses regarding possible ways of tuning the pathway activation threshold. A simple deterministic model of the G protein cycle [16] is presented next. This model was chosen for its simple but precise structure and adopted in the derivation of a tractable kinetic model of the full pathway.

The new pathway model presented herein share the structure of the simple G protein cycle reported elsewhere and extends it to include other modules and higher order kinetics. The designed model was used for the purpose of investigating the mechanism of the pathway activation.

For simulating biochemical processes involved in this system, both stochastic and deterministic approaches were used (see Sec. A) for details).

3.1 Nomenclature

Nomenclature of the system variables and reaction rates presented in this section will be further used in the sequel.

R	Inactive Ste2 receptor
RL	Activated Ste2 receptor with bounded pheromone
G	G protein, inactive in it's heterotrimeric state
Ga	Active Gα-GTP
Gbg	Active G$\beta\gamma$ subunit
Gd	Inactive Gα-GDP
$Sst2$	Sst2
r_{RL}	Pheromone-receptor binding
r_{RLm}	Pheromone-receptor dissociation
r_R	Ste2 synthesis
r_{dR}	Ste2 degradation
r_{dRL}	Receptor with pheromone degradation
r_E	GDP exchange rate

r_H GTP hydrolysis rate
r_{bg} Rate of G$\beta\gamma$ and Gα-GDP re-association
r_M Rate of MAPK activation

3.2 Complex stochastic model

In publication [13], a complex model of the whole yeast pheromone pathway is presented with the BioNetGen code of the model available in supplementary material. Within this work, the model helped with defining the important concepts regarding the dose response and it was used for analysing possible ways of regulating the receptor activation while focusing on the Sst2 action.

This very detailed model of the real system describes the pathway from the binding of the pheromone to the Ste2 receptor and it ends with activation of the Ste12 transcription factor. The model works with 28 species and 272 reaction rules representing the majority of chemical reactions known to occur. Using Gillespies's stochastic simulation algorithm (SSA) for simulating Markov Chain models, the temporal changes in numbers of molecules are generated.

The model dose-response has been shown to fit experimental data in [13]. Therefore in subsequent modelling developments, this model was taken to represent the actual system behaviour. In Fig. 5, there is a comparison of simulation outputs with some experimental data that show that the model fits dose-response behaviour of the real system. In order to obtain a dose-response curve characterising the modelled system, its behaviour was simulated for the pheromone input in logarithmic range from 10^{-4} nM to 10^3 nM. The output was measured in concentration of active Fus3 which is one of the possible measurable outputs for characterising the pathway activation (see Sec. 4.1 for details). The data from simulations fit the experimental data.

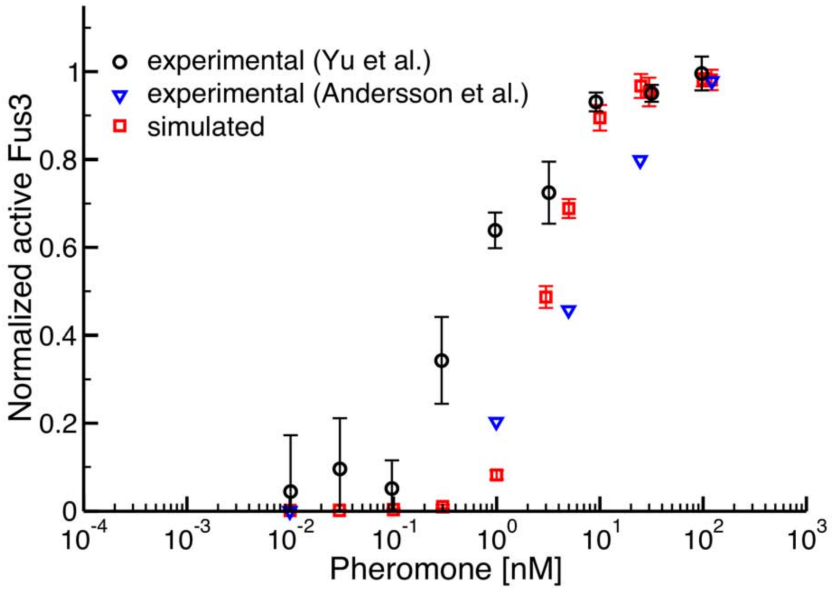

Figure 5: Red rectangles are the simulation outputs in form of active Fus3. Model behaviour was simulated for series of input amounts of α-factor that correspond to concentration of α-factor that was cell exposed to, as it was in experiments - black circles [1] and blue triangles [17]. This figure is taken from [13].

The following section describes the reaction involving Sst2 within the complex pathway model. The effect of Sst2 concentration on pathway activity is also shown.

3.2.1 Model of the Sst2 action

Reactions describing the Sst2 behaviour in this model include basal Sst2 synthesis and also a pheromone induced transcription through Ste12. Sst2 is phosphorylated by active Fus3 and it degrades more rapidly in the phosphorylated than in the unphosphorylated state. This is modelled according to [8] who proposed that Sst2 degrades more rapidly after pheromone exposure due to its ubiquitination. Sst2 binds Ste2 with Gpa1 and accelerates the Gpa1-GTP hydrolysis in phosphorylated and unphosphorylated states equally.

Series of simulations were performed in order to analyse the pathway behaviour for various Sst2 levels.

3.2.2 The Sst2 assay simulations

Simulation of the model represents the pathway response to an input pulse of α-factor. One run corresponding to 4000 s takes about 25min CPU time.

A series of simulations were performed in order to obtain dose-response curves of the system with varying Sst2 expression rates producing various Sst2 concentrations in each simulation. For each Sst2 synthesis rate, the model behaviour was simulated for 20 different input amounts of α-factor in logarithmic range from 10^{-1} nM to 100 nM and the corresponding levels of active Fus3 were measured as an output (the same output as in Fig. 5). The dose response curves are plotted in Fig. 6. The results indicate that the Sst2 expression levels have direct impact on pathway activation. The activation threshold moves to lower pheromone levels with decreasing Sst2 levels and vice versa. In the figure, the wild-type graph is identical to the validated graph in Fig. 5. Note the low expression rate shows hypersensitivity to pheromone in agreement with published results for Sst2 knockout mutants [16] [5].

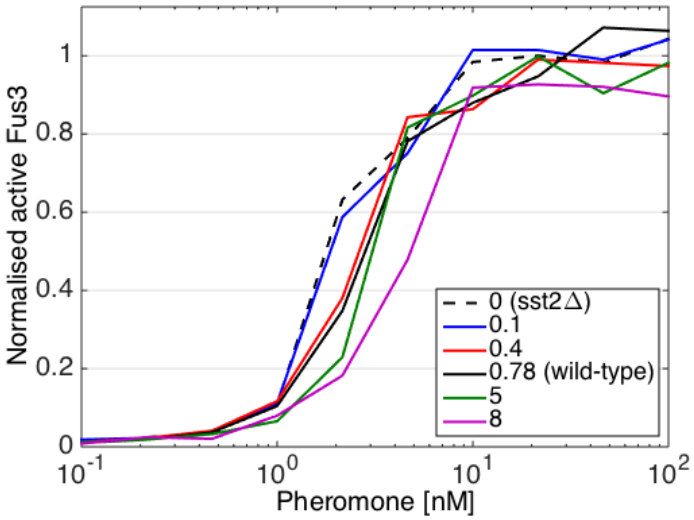

Figure 6: Simulation results show that for lower Sst2 expression levels

These simulation results suggest that it is possible to tune the pathway activation by varying the Sst2 levels. The mechanism by which the threshold is modulated is however unclear. Hence the conditions where this trend holds are also unclear. A simpler model is therefore required. Such model is derived in the next section.

3.3 Simple structural model

For further investigation of the Sst2 action was desired to use a model that focuses on the interaction between Sst2, G protein and Ste2. A simple deterministic model was presented by Yi et al. in [16] that clearly describes the G protein cycle. Yi model has a simple but correct structure that was further adopted for designing a kinetically more precise model. This section describes a model that was introduced in [16] and everything presented in this section is work of the authors of the paper. Nevertheless, it is necessary to explain their model in detail because it is fundamental for understanding further model developments of this work.

The deterministic model is represented by ODEs that were obtained by applying the law of mass action. Since the variables in Yi model are concentration in molecules per cell, the model simulation results can be directly compared to the stochastic model simulations that generates also numbers of molecules.

3.3.1 System structure

In the model (Fig. 7), Ste2 receptor (R) is exposed to a constant level of pheromone - ligand (L). The pheromone binds the receptor and activates it. The receptor-ligand binding has rate r_{RL} and spontaneous receptor-ligand dissociation has rate r_{RLm}. Active receptor (RL) induces GDP-GTP exchange on Gα subunit within the heterotrieric G protein (G) and the G protein dissociates. It releases active forms of both its subunits Gα-GTP and G$\beta\gamma$. The exchange rate is r_E. Sst2 catalyses GTP hydrolysis within Gα-GTP and it deactivates the Gα subunit. The hydrolysis rate is r_H. Inactive Gα-GDP reassociates with the G$\beta\gamma$ subunit to reconstitute the heterotrimer where the both subunits are inactive. Rate of G protein reassembly has rate r_{bg}. The model includes both synthesis and degradation of Ste2 and also degradation of Ste2 with bounded pheromone. The rates are r_R, r_{dR}, r_{dRL}, respectively. The total number of G proteins and Sst2 are assumed constant.

This model does not consider that different Sst2 levels could change the model dynamics. The Sst2 action is only included in the reaction rate constant for GTP exchange that only differs for Sst2 null mutants (basal GTPase activity in absence of Sst2).

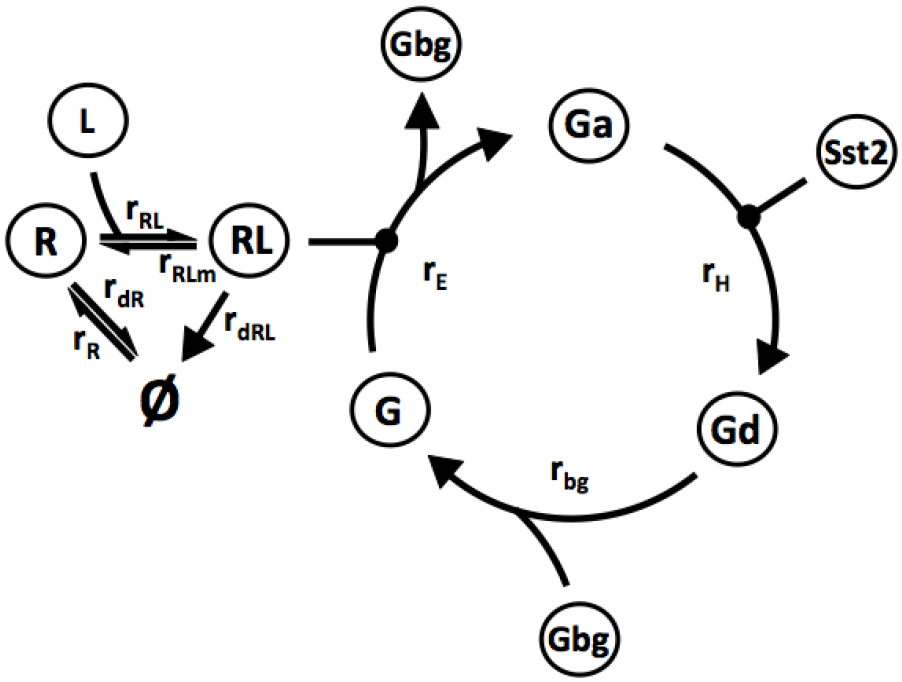

Figure 7: Schematic of the system structure [16].

The system can be completely described by defining the behaviour of the state variables R, RL, G, and Ga. The temporal changes of their concentrations (square brackets stand for concentrations) are written by reaction rates corresponding to the schematic in Fig. 7:

$$\frac{d[R]}{dt} = -r_{RL} + r_{RLm} - r_{dR} + r_R \tag{1}$$

$$\frac{d[RL]}{dt} = r_{RL} - r_{dRL} \tag{2}$$

$$\frac{d[G]}{dt} = r_{bg} - r_E \tag{3}$$

$$\frac{d[Ga]}{dt} = r_E - r_H \tag{4}$$

Assuming the total number of G proteins per cell is constant and equal to Gt, the remaining two state variables can be computed using the following conservation laws:

$$[Gbg] = Gt - [G], \tag{5}$$

which says that the total number of G proteins is equal to sum of free G$\beta\gamma$

subunits and G$\beta\gamma$ subunits bound to Gα in the form of the heterotrimer. Second conservation law says that that sum of active and inactive Gα subunits is equal to the free G$\beta\gamma$ subunits:

$$[Gd] = Gt - [G] - [Ga]. \tag{6}$$

It is in agreement with fact that one heterotrimeric G protein dissociates to one Gα and one G$\beta\gamma$ subunit.

Within the publication, the model was validated in terms of its dose response (Fig. 8). The model behaviour was simulated for pheromone input levels in range from 10^{-3} nM to 10^{3} nM and corresponding levels of Ga were measured at the time point 60 s. Simulation results were compared with measured G protein activation from three independent experiments for various pheromone inputs in the range from 0.1 nM to 100 nM. Despite the simplification of the model, simulation data fit the dose-response curve of experimental data.

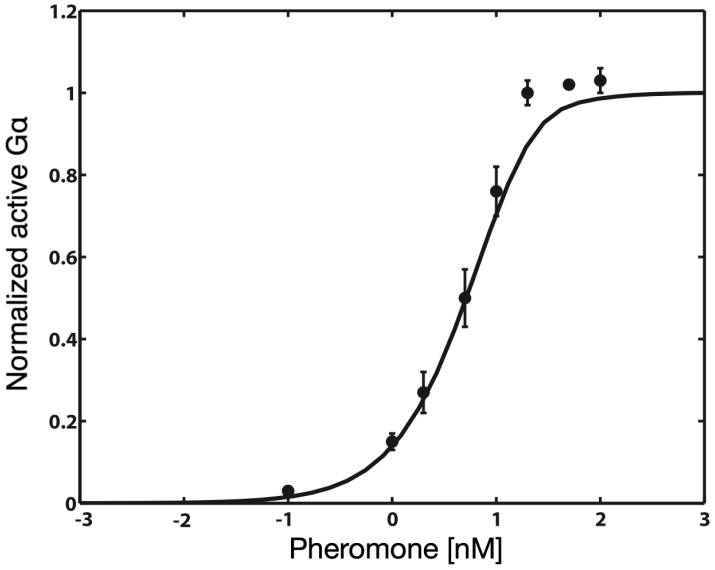

Figure 8: Dose response curve with data from experiments (dots) and simulations (black line). Data were normalized to the output value at 1 μM α-factor [16]. This figure was taken from [16].

Although this model is simple, clear, and correct in sense of pathway response it neglects some important kinetics. Sst2 action, which is fundamental in defining the Ste2 receptor activation mechanism, is simplified. Therefore, this model as it is

cannot be used for the purpose of investigating the system's behaviour for different Sst2 levels. Thus, only its structure and some of the kinetics were adopted for the design of a new model that later allows analysis of the Sst2 tuning mechanism.

3.4 Derived kinetic model

For the first time, a model that presents precise Sst2 kinetics is introduced within this work. The designed model build on the Yi model presented above. It uses the same structure and state variables but it introduces higher order kinetics omitted from the Yi model.

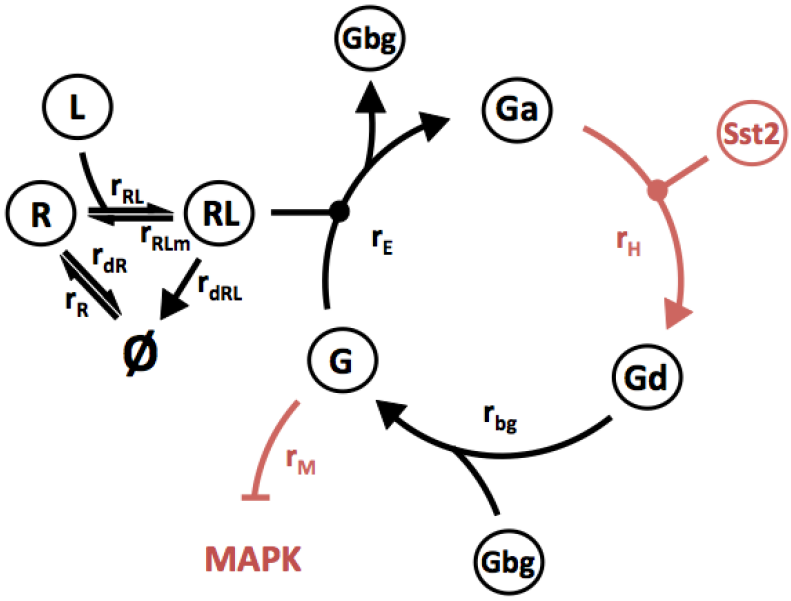

Figure 9: Schematic of the designed model. Black arrow rates have dynamics preserved from the Yi model, red arrows correspond to dynamics that were added or changed.

Fig. 9 presents the extended model structure. Reactions with black arrows are identical with the model presented by Yi, red arrows correspond to reactions that were added or that are modelled differently. The mechanism of the Ste2-pheromone binding and the structure of the G protein cycle are preserved, but the key factor - Sst2 kinetics - is modelled differently to better reflect the reality (see eg. [3] for Gpa1-Sst2 binding and activation mechanism). This model extends the Yi model to include the entire pathway with additional rate that represents the

MAPK cascade activation. Note, the parameter values are not important for the analysis in this section. For later comparison with earlier models the parameter values in Sec. B were used.

3.4.1 Mathematical model

The same as in Yi model, the Ste2 receptor is exposed to a constant level of pheromone α-factor. The pheromone binds the Ste2 receptor and activates it

$$R + L \rightarrow RL. \qquad (r_{RL})$$

Spontaneous dissociation of receptor with ligand is included

$$RL \rightarrow R + L. \qquad (r_{RLm})$$

Both Ste2 formation and degradation is included

$$\emptyset \rightarrow R, \qquad (r_R)$$

$$R \rightarrow \emptyset, \qquad (r_{dR})$$

and also degradation of receptor with bound pheromone is included

$$RL \rightarrow \emptyset. \qquad (r_{dRL})$$

Kinetics of these reactions are preserved from the Yi model and are modelled according to mass action kinetics (see Sec. A.1):

$$\begin{aligned} r_{RL} &= k_{RL}[L][R], && (7)\\ r_{RLm} &= k_{RLm}[RL], && (8)\\ r_R &= k_{Rs}, && (9)\\ r_{dR} &= k_{Rd0}[R], && (10)\\ r_{dRL} &= k_{Rd1}[RL]. && (11) \end{aligned}$$

Activated receptor bound to G protein heterotrimer induces GDP-GTP exchange on its Gα subunit and dissociation of the active Gα-GTP and G$\beta\gamma$ subunits

$$G \rightarrow Ga + Gbg. \qquad (r_E)$$

This reaction is also preserved from the Yi model and is modelled according to mass action kinetics. The exchange rate is

$$r_E = k_{Ga}[RL][G]. \qquad (12)$$

Active Gα-GTP binds Sst2 and the Sst2 accelerates GTP hydrolysis on Gα subunit. Hydrolysis is modelled as an enzymatic reaction in this model where Sst2 binds Gα-GTP and forms a complex, catalyses GTP hydrolysis and dissociates:

$$Sst2 + Ga \rightleftharpoons Sst2Ga \rightarrow Sst2 + Gd. \qquad (r_H)$$

As far as the enzyme ($Sst2$) concentration is constant and much less than the substrate (Ga) concentration, according to Michaelis-Menten kinetics (Sec. A.1), the hydrolysis rate is

$$r_H = \frac{k_{Gd1}[Sst2][Ga]}{(\frac{k_H^D}{[Ga]})^{nH} + 1} + k_{Gd0}[Ga], \qquad (13)$$

where k_H^D is dissociation constant and k_{Gd0} is the rate of basal GTPase activity. The Hill coefficient n_H represents cooperativity. This reaction is modelled differently than in the Yi model where the Sst2 impact is only included in reaction rate constant k_{Gd1} that is assumed grater than the reaction rate k_{Gd0} in absence of the Sst2 protein

$$Ga \rightarrow Gd, \qquad (r_H)$$

with the rate

$$r_H = k_{Gd1}Ga \qquad (14)$$

for wild-type cell, and

$$r_H = k_{Gd0}Ga \qquad (15)$$

for null mutant that both have the kinetics definitely different from the enzymatic rate.

Product of the enzymatic reaction is inactive Gα-GDP that can bind G$\beta\gamma$ to reform the heterotrimer. This reaction is also preserved from the Yi model and modelled according to mass action (Sec. A.1). Its rate is

$$r_{bg} = k_{Gd}[Gd][Gbg]. \tag{16}$$

When G$\beta\gamma$ is dissociated from the Gα subunit it is in its active state. It further activates the MAPK cascade until it associates with Gα-GDP and becomes inactive. Then, when bound to $G\alpha$-GDP, it blocks the MAPK cascade activation. Therefore, rate of MAPK activation was added that represents the pathway downstream response after pheromone exposure. In the model, MAPK is repressed by $[G]$ - the inactive form of G$\beta\gamma$. Yi model does not include this downstream portion of the pheromone response.

The MAPK cascade results in Fus3 activation that can be presented by the reaction

$$Fus3 \rightarrow Fus3^* \qquad (r_M)$$

which is catalysed by G$\beta\gamma$ (equivalently repressed by G). The MAPK cascade kinetics can by approximated by the following Hill function:

$$r_M = \frac{k_M}{1 + (\frac{[G]}{k_M^D})^{nM}}, \tag{17}$$

where k_M^D is the dissociation constant and k_M is the maximum rate of MAPK activation. Hill coefficient n_M represents cooperativity. MAPK activation represents another measurable output that can be used in simulations.

This model was designed in order to investigate the system's behaviour leading up to the MAPK activation. Therefore, all possible pheromone-dependent transcriptional activation and degradation can be omitted [11]. The Sst2 concentration is assumed constant within a single simulation. The total number of G proteins is constant throughout all simulations. As a result, conservation laws (5) and (6) as they were established by Yi are still valid.

The model is described by four non-linear ODEs with the same state variables used in the Yi model. The variables represent the species' concentrations in

molecules per cell, the pheromone input [L] is in molar concentration.

$$\frac{d[R]}{dt} = -k_{RL}[L][R] + k_{RLm}[RL] - k_{Rd0}[R] + k_{Rs} \quad (18)$$

$$\frac{d[RL]}{dt} = k_{RL}[L][R] - k_{RLm}[RL] - k_{Rd1}[RL] \quad (19)$$

$$\frac{d[G]}{dt} = k_{Gd}[Gd][Gbg] - k_{Ga}[RL][G] \quad (20)$$

$$\frac{d[Ga]}{dt} = k_{Ga}[RL][G] - \frac{k_{Gd1}[Sst2][Ga]}{(\frac{k_H^D}{[Ga]})^{nH} + 1} + k_{Gd0}[Ga] + k_{Gd0}[Ga] \quad (21)$$

Structure of the model is the same as in the Yi model but the newly introduced kinetics allow analysis of the system behaviour for various Sst2 concentrations.

3.5 Characterization of pathway activation

In this section, the relationship between the Ste2 receptor activation and the concentration of the Sst2 is mathematically derived. It is shown that it is possible to move the pathway activation threshold (Fig. 5) simply by varying the Sst2 levels under certain assumptions. Specifically it is shown that if the activation threshold for Sst2 is lower than the activation threshold for the MAPK, and if the leaky rate of the hydrolysis is low, then the activation of the entire pathway is controlled by the Sst2 concentration.

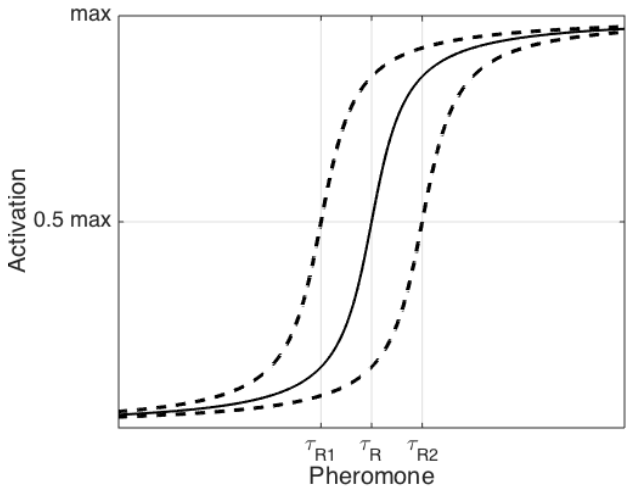

Figure 10: Receptor activation threshold is the point of reaching the half maximum activation.

For following analysis, the kinetics of hydrolysis (r_H) and the MAPK activation (r_M) can be interpreted in sense of activation thresholds. For any enzymatic reaction, the activation threshold K_d (Sec. A.1) is the concentration of substrate required to achieve 50% of the maximum rate. Thus, the Sst2 activation threshold k_H^D corresponds to the concentration of Ga required to achieve 50% of the r_H maximum. The activation threshold of MAPK k_M^D is the concentration of G required to achieve 50% of the r_M maximum. Both k_M^D and k_H^D contribute but are not equivalent to whole pathway activation. The pathway activation threshold is the pheromone concentration required to achieve 50% of the maximum pathway activation. Below, the temporal order of activation events corresponding to Sst2, MAPK, and the pathway is derived.

To enable analytic solution, r_H and r_M are approximated by step or pseudo-step functions. This is equal to letting the Hill coefficient $n_H,\ n_M \to \infty$. The hydrolysis rate given by the kinetics in (13) then has the following form:

$$r_H = \begin{cases} k_{Gd0}[Ga] & \text{for } [Ga] < k_H^D \\ k_{Gd1}[Sst2] & \text{for } [Ga] \geq k_H^D. \end{cases} \tag{22}$$

Similar the MAPK rate has the form below:

$$r_M = \begin{cases} k_M & \text{for } [G] < k_M^D \\ 0 & \text{for } [G] \geq k_M^D, \end{cases} \tag{23}$$

Qualitatively these rates are illustrates in Fig. 11.

For the purpose of analysis, the system is considered in equilibrium. In chemical equilibrium, the kinetics achieve steady state and the rates within the G protein cycle are equal

$$r_E = r_H = r_{bg}. \tag{24}$$

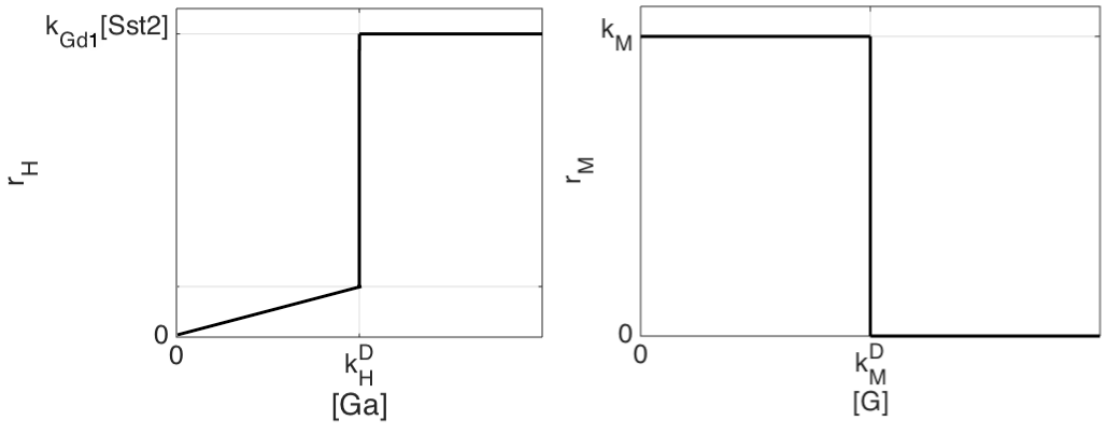

Figure 11: Approximation of the r_H reaction rate and r_M reaction rate for $n_H = n_M = \infty$ (B).

These two simplifications - the state of equilibrium together with the approximation of the rates' kinetics - enable analysis of the system behaviour in terms of activation thresholds. Two scenarios are considered:

- Scenario 1: When pheromone concentration reaches the activation threshold, Sst2 is active.
- Scenario 2: When pheromone concentration reaches the activation threshold, Sst2 is not active.

Subsequently, the pathway activation thresholds of Scenario 1 ($k^D_{P,1}$) and Scenario 2 ($k^D_{P,2}$) are compared and the conditions when $k^D_{P,1} < k^D_{P,2}$ are derived. Lastly it is shown, that $k^D_{P,1}$ is proportional to the concentration of the Sst2.

Scenario 1

- Derivation of upper limit on $k^D_{P,1}$

  The concentration of active Ste2 ($[RL]_H$) at the point of MAPK activation is derived.

  Fact 1.

$$[RL]_H = \frac{k_{Gd0} k^D_H}{k_{Ga} k^D_M}, \tag{25}$$

Proof. At the point of Sst2 activation, the hydrolysis rate is

$$r_H = k_{Gd0}[Ga], \tag{26}$$

and the exchange rate is

$$r_E = k_{Ga}[RL]_H[G]. \tag{27}$$

From chemical equilibrium (24)

$$r_H = r_E, \tag{28}$$

the expression (25) is derived. The result follows

$$[Ga] = k_H^D, \text{ and } [G] \geq k_M^D. \tag{29}$$

Hence,

$$k_{P,1}^D \leq [RL]_H \leq \frac{k_{Gd0}k_H^D}{k_{Ga}k_M^D}. \tag{30}$$

□

Scenario 2

- Derivation of $k_{P,2}^D$

  The concentration of active Ste2 ($[RL]_M$) at the point of MAPK activation is derived. Throughout, it is assumed that Sst2 is not active.

  Fact 2.

$$[RL]_M = \frac{k_{G1}(Gt - k_M^D)^2 k_{Gd0}}{k_{Ga}k_M^D(k_{Gd0} + k_{G1}(Gt - k_M^D))}, \tag{31}$$

  Proof. By the conservation laws (5) and (6) , Gbg at the point of MAPK activation is

$$[Gbg] = Gt - k_M^D, \tag{32}$$

$$[Gd] = Gt - [Ga] - k_M^D. \tag{33}$$

  By setting

$$r_E = r_H, \tag{34}$$

Ga can be computed analytically:

$$Ga = \frac{k_{Ga} k_M^D [RL]_M}{k_{Gd0}}. \tag{35}$$

Substituting these relations, the rate of r_{bg} is given by

$$r_{bg} = k_{G1}(Gt - \frac{k_{Ga} k_M^D [RL]_M}{k_{Gd0}}) - k_M^D)(Gt - k_M^D). \tag{36}$$

The result follows from solving for $[RL]_M$ in the equation

$$r_E = r_{bg}. \tag{37}$$

The pathway threshold is relayed to $[RL]_M$

$$k_{P,2}^D = [RL]_M. \tag{38}$$

□

Next, $k_{P,1}^D$ and $k_{P,2}^D$ are compared.

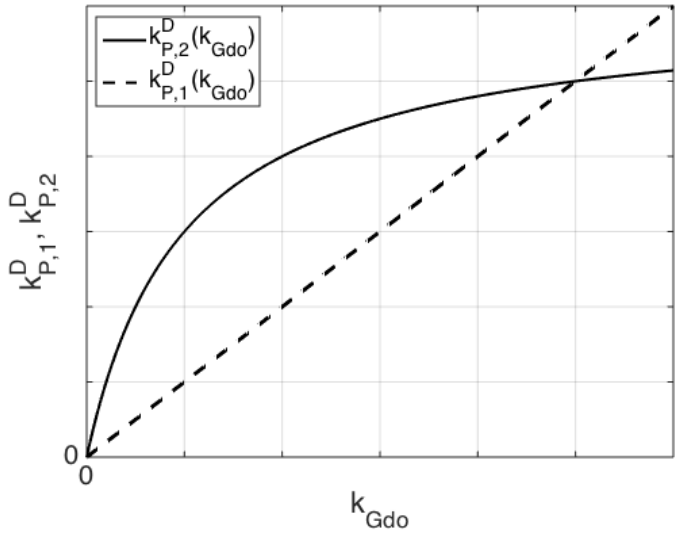

Figure 12: The behaviour of the dissociation constant as functions of leaky hydrolysis k_{Gd0}

By inspection of Fig. 12 is clear that $k^D_{P,1} < k^D_{P,2}$ if and only if

$$\frac{d\ k^D_{P,1}}{d\ k_{Gd0}} < \frac{d\ k^D_{P,2}}{d\ k_{Gd0}}. \tag{39}$$

From Fact 1 and Fact 2 follows

$$\frac{d\ k^D_{P,1}(k_{Gd0})}{d\ k_{Gd0}} = \frac{k^D_H}{k^D_M k_{Ga}} \tag{40}$$

$$\frac{d\ k^D_{P,2}(k_{Gd0})}{d\ k_{Gd0}} = \frac{Gt - k^D_M}{k^D_M k_{Ga}} \tag{41}$$

Fact 3. *For k_{Gd0} sufficiently small, the Sst2 is active at the point of the pathway activation if and only if*

$$k^D_H < Gt - k^D_M. \tag{42}$$

Finally, the dependence of $k^D_{P,1}$ on Sst2 is derived.

Fact 4.

$$k^D_{P,1} = \frac{k_{Gd1}[Sst2]}{k_{Ga} k^D_M} \tag{43}$$

Proof. At the point of the pathway activation, the concentration of active Ste2 is $k^D_{P,1}$. Substituting it for $[RL]$ into the expression for r_E and substituting

$$G = k^D_M, \tag{44}$$

the result follows from solving for $k^D_{P,1}$ in the equation

$$k_E = k_H, \tag{45}$$

where

$$k_H = k_{Gd1}[Sst2]. \tag{46}$$

□

Hence, the pathway activation threshold depends linearly on the concentration of Sst2.

It was shown that it is possible to tune the pathway activation threshold by varying the Sst2 levels, assuming that the leaky hydrolysis is low and that the activation threshold of Sst2 is lower than the activation threshold of MAPK.

3.6 Simulations

Series of simulations were performed in order to support the statement about the model behaviour introduced in previous section - that the pathway activation threshold can be tuned only by varying the Sst2 levels under the assumptions that the Sst2 is activated before the MAPK cascade and that the leaky hydrolysis rate is sufficiently small.

First, the model was validated in sense of dose-response. Same as in [16], the output in the form of active Gα was measured for a logarithmic range of input pheromone concentrations from 0.01 nM to 1 μM in order to obtain dose-response curve of the system. The same experimental data as in Fig. 5 and experimental data from Fig. 8 were used as reference for comparison with the simulated data. The designed model fits the experimental data, especially the data from [1].

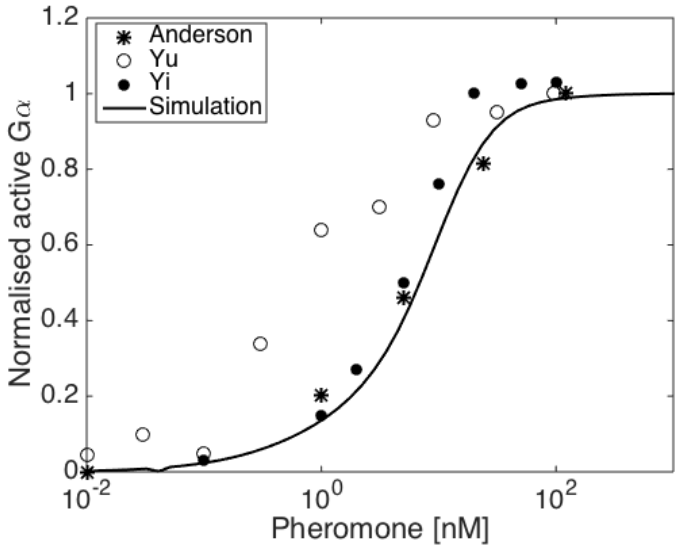

Figure 13: Simulated data (solid line) are comared with experimental data from three different publications: stars [1], circles [17], and dots [16].

Below is an example of a single simulation run following exposure to a constant level of pheromone. In Fig. 14, the response of the four state variables to a step input corresponding to 100 nM pheromone concentration is plotted.

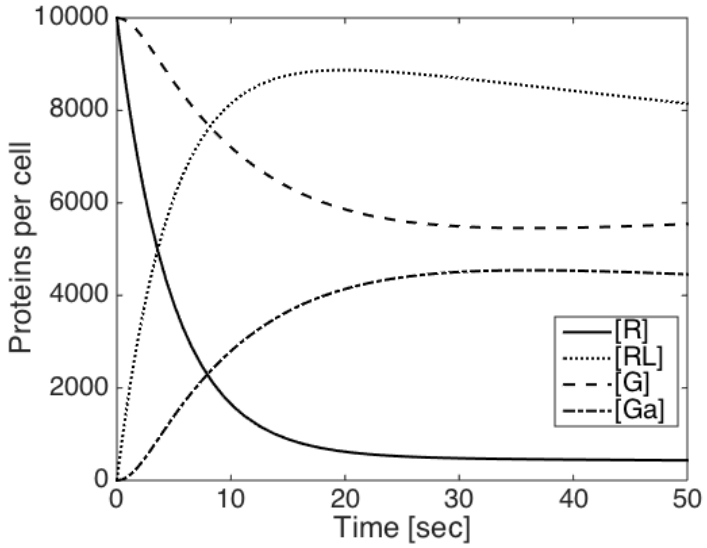

Figure 14: One simulation responses.

The system dynamics are quite fast in the beginning of the simulation. Nearly all receptors are quickly occupied by pheromone resulting in sharp increase in $[RL]$ and decrease in $[R]$. G protein dissociation follows and $[Ga]$ increases together with decrease in $[G]$ enabling activation of the MAPK cascade.

In Fig. 15, there are shown the r_H and the r_M kinetics with the corresponding substrate behaviours. For given activation thresholds that are displayed in the plots, the Sst2 is activated before the the MAPK cascade. Values used in simulations are

$$\begin{aligned} k_H^D &= 2000 \\ k_M^D &= 7000 \\ Gt &= 10000 \\ n_M &= 2 \\ n_H &= 2, \end{aligned}$$

which completes the requirement for the Sst2 being activated before the MAPK cascade

$$k_H^D < Gt - k_M^D. \tag{47}$$

The values of k_H^D and k_M^D were chosen to fit the data. Most of the other model

parameters such as reaction rates and total protein amounts are taken from various publications where they were experimentally determined (see Table B).

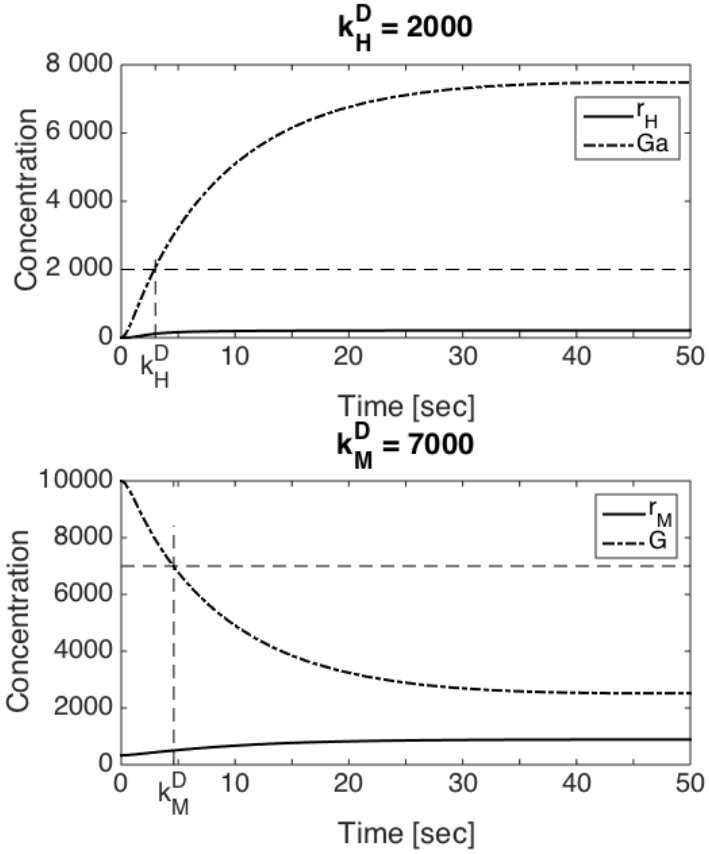

Figure 15: Sst2 is activated before the MAPK cascade.

Simulation of the Sst2 assay was performed in order to obtain dose-response curves for various Sst2 levels. The resulting 3-D plot (Fig. 16) is in agreement with the statement introduced in Sec. 3.5: Assuming that Sst2 is activated before MAPK cascade, the pathway can be tuned only by varying the Sst2 levels.

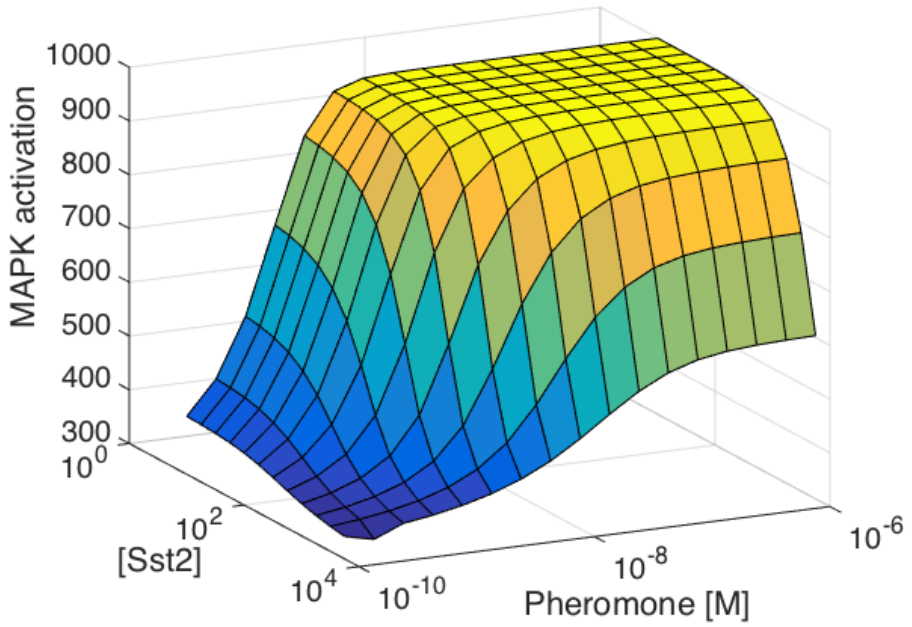

Figure 16: Simulation results confirm that receptor activation can be tuned by varying the Sst2 levels.

Decreasing Sst2 concentration moves the pathway activation threshold towards the hypersensitivity to pheromone and vice versa. It also means that for higher Sst2 concentration, higher pheromone input is required to activate the pathway. On the other hand, for very low Sst2 concentration, even low pheromone input is enough to activate the pathway. Taken all together, the results confirm that assuming that the Sst2 is activated before the MAPK cascade and with low leaky hydrolysis, the receptor activation can be tuned by varying the Sst2 concentration.

4 Experimental validation

The process of experimental validation of the model is designed to study the receptor activation for varying Sst2 levels *in vivo*. Within the experiments, the Sst2 concentration in cells is variable and its relative concentration is measured, and the pathway response for various α-factor inputs is determined. Following section summarises some methods for measuring the pathway response experimentally.

4.1 Dose-response measurement methods

As already mentioned in Sec. 3, dose-response curve shows the input-output behaviour of the receptor. There are more ways of measuring the pathway activation and there is a proportional relationship between the curves obtained by different measurements. Authors of [16] have shown that four different dose-response curves overlap after normalisation: receptor affinity, G protein activation, pheromone-dependent transcriptional induction, and cell-cycle arrest (Fig.17).

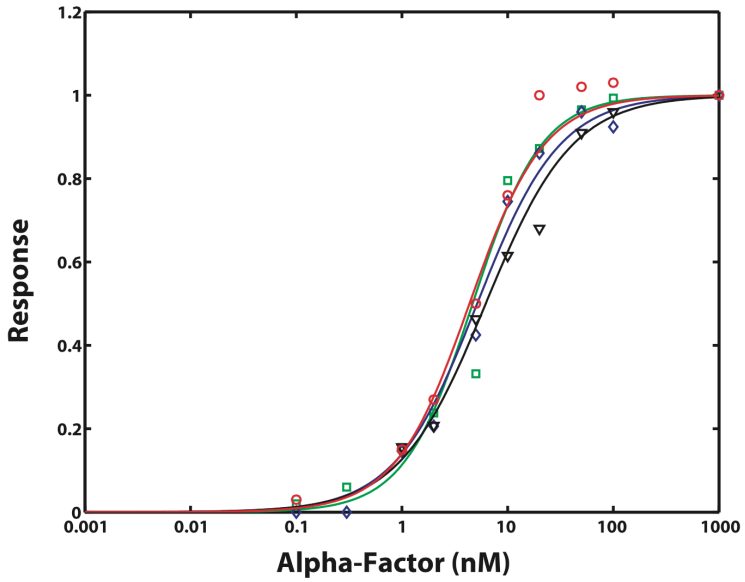

Figure 17: Authors of [16] measured four different dose-response curves: receptor affinity (black triangles), G protein activation (red circles), transcriptional induction of pFUS1-GFP (green squares), and cell-cycle arrest (blue diamonds). This figure was taken from [16].

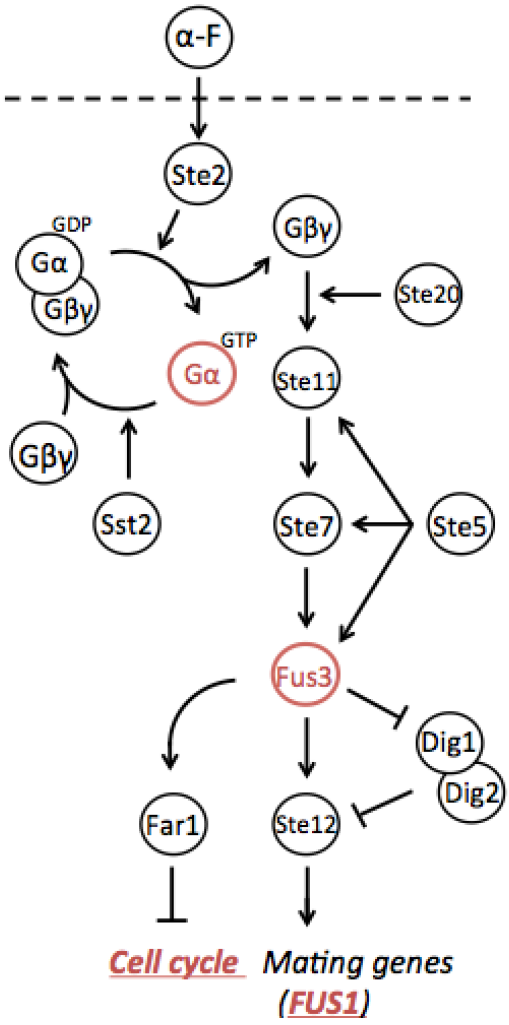

Figure 18: Components of yeast pheromone pathway that are often measured as an output for a dose-response curve are denoted in red.

Following are frequently used methods for measuring the pathway activation (in Fig. denoted in red).

G protein activation The output from measuring G protein activation is relative amount of active Gα (and G$\beta\gamma$) subunits.

Fus3 activity Measuring Fus3 activity corresponds to measuring relative amount of phosphorylated (active) Fus3, the mitogen-activated kinase.

Transcriptional induction The concentration of one of the mating genes product (mostly it is Fus1) is measured after pheromone exposure. Mating genes are transcriptionally induced by phosphorylated Ste12.

Cell-cycle arrest Simultaneously with mating induction, cell cycle is arrested. Growth inhibition of liquid culture is observed after adding α-factor into a culture of cells. OD (optical density) of the liquid culture is measured which corresponds to relative amount of cells in the medium.

Growth curves from all these types of measurements overlap after normalisation. It suggests proportional relationship between these downstream activations [16] [17]. Therefore any of the methods can be used for measuring dose-response curves. Measuring cell-cycle arrest is probably the easiest method since it only requires performing an OD assay.

4.2 Materials and methods

Strains and plasmids Strains used in this study are wild-type BY4741 (*MATa his3Δ1 leu2Δ0 met15Δ0 ura3Δ0*) and its sst2 knockout (*MATa his3Δ1 leu2Δ0 met15Δ0 ura3Δ0 sst2Δ::kanMX4*), both gift from Samson lab, MIT [14]. The wild-type strain and the *sst2*Δ strain were used as controls in the assays, when the wild-type strain with its Sst2 levels exhibit normal behaviour in sense of dose-response, and the knockout exhibit extreme behaviour since it has no Sst2 at all. For the purpose of measuring the responses for various Sst2 concentrations, the knockout strain was transformed with plasmid carrying GFP-tagged SST2 gene on an inducible GAL1 promoter[1] creating *SST2*$^+$ strain.

Vector pRS416 carries genomic SST2 fused to yEGFP (yeast-optimised GFP) on genomic GAL1 promoter. The plasmid was constructed using Gibson assembly that combined two fragments - vector carrying pGAL1-GFP with CYC1 terminator and genomic SST2 with a linker that was added by PCR.

GAL1 promoter activity is dependent on amount of glucose present. Glucose is added to the liquid culture of cells and activates the promoter. In some range, the GAL1 promoter activity is proportional to the amount of glucose in medium until the promoter activity saturates. SST2 gene that follows GAL1 promoter produces

[1]Promoter is a regulatory part of DNA that regulates the amount of protein produced from following gene.

Sst2 protein tagged with GFP (green fluorescent protein). It means each molecule of the Sst2 produced has a bond to a molecule of GFP. After excitation by UV light, GFP emits observable green light. As a result, relative amount of Sst2 can be monitored by measuring fluorescence.

Dose response measurements Cells were grown in 30°C for two days in minimal medium with 2% sucrose supplemented with appropriate amino acids. After two days, cells were spinned down and re-suspended in a fresh medium. After another day of growth, cells were spinned down and resuspended in minimal medium supplemented with appropriate amino acids and various concentrations of galactose filled up with sucrose to keep the sugar concentration in medium 2%. After 3 hours, which is a time needed for GAL1 induction, various amounts of α-factor were added. Within the following 6 hours, OD was measured and from resulting OD plots, growth arrest can be evaluated.

The samples were cultivated in clear flat bottom black 96-well plates enabling measuring OD and fluorescence simultaneously. The *SST2*$^+$ strain and the controls were cultivated in 0% and 2% galactose media in three replicates with α-factor and in three replicates without the α-factor. The α-factor concentrations used were 100 nM, 1 μM, and 10 μM.

Resulting plots show the growth arrest of cells exposed to pheromone relative to growth of cells with no pheromone. For each of the samples, the OD time-curve is normalised to initial value 0.1 and an average is computed from the replicates. The relative growth is computed as an average OD of cells with the α-factor divided by an average OD of cells without the α-factor. These values are computed for four different samples: wild-type strain, *sst2*Δ and *SST2*$^+$ in two different galactose concentrations.

4.3 Results

Plasmid verification The plasmid constructed for the purpose of the experimental validation was verified on gel after restriction with XhoI and BamHI that are on the sides of the insert. Three samples out of the four on gel in Fig. 19 have the correct bands of 4.8 kb and 3.6 kb.

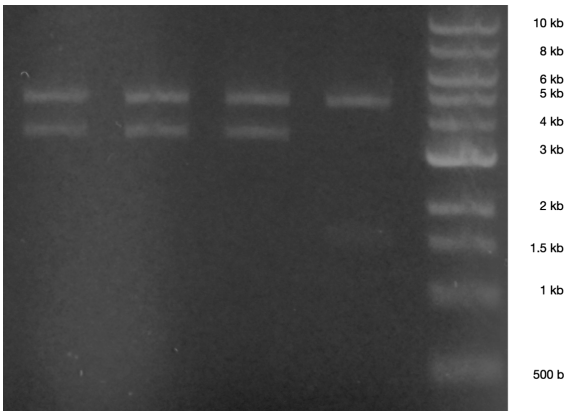

Figure 19: Three from the four samples confirm the successful assembly of the plasmid.

GAL1 promoter characterisation Prior to the experiments itself, the GAL1 promoter activity was characterised. It provides the necessary information about the regulatory unit by which the Sst2 concentration is controlled. The information about the time needed for the full promoter induction was determined from the data shown in Fig. 16.

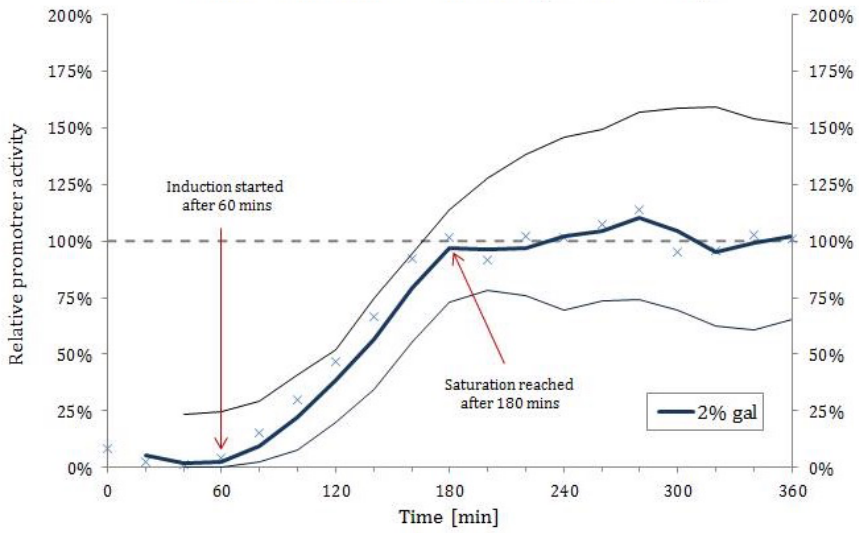

Figure 20: Characterisation of pGAL1 activity.

The data show that the promoter is fully activated after 3 hrs of incubation with galactose. Thus in the Sst2 assays, the samples were incubated for 3 hrs with galactose added and then the α-factor was added and OD started to be measured.

Dose-response measurement assays The temporal changes of relative growth of the culture in 10 μM pheromone concentrations are plotted in Fig. 21. In time corresponding to $t = 0$ *min* in the figure, the culture has already been induced by galactose for 3 hrs, and the α-factor was just added. The dots correspond to mean values from three replicates with corresponding errorbars and they are extrapolated by linear functions.

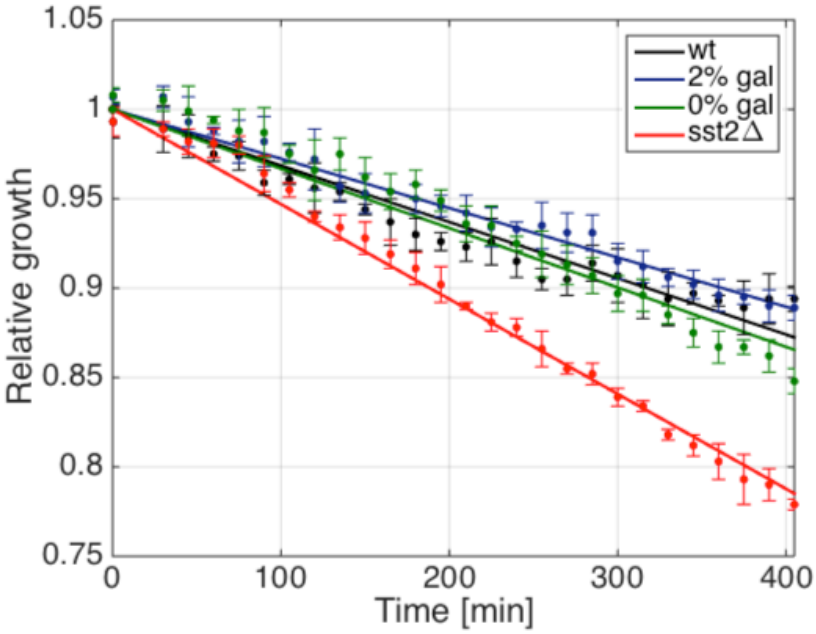

Figure 21: Relative growth of cultures exposed to 10 uM of α-factor.

Put these data together with the data for concentrations of 100 nM and 1μM (data not shown), the rough dose-response curves for various Sst2 concentrations and the controls are shown in Fig. 22.

In the experiment, the Sst2 levels correspond to the levels of galactose in the medium. According to the model, the activation thresholds would be the lowest for the knockout strain (sst2Δ) and zero galactose induction (0% gal), then higher

for 2% galactose induction (2% gal) and the wild-type strain (wt). The values plotted in Fig. 22 are slopes of the linear data approximations from Fig. 21.

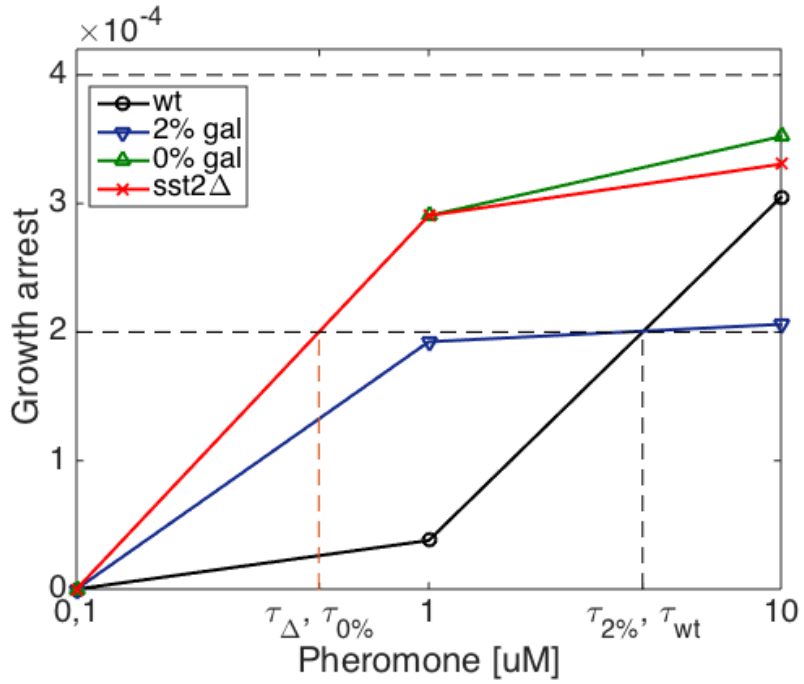

Figure 22: Dose response curves of the strains measured for three different pheromone inputs.

Unfortunately, the pheromone concentration of 10 μM was not sufficient for the pathway activation to saturate for all the samples, therefore it is not possible to determine the pathway activation thresholds from these data precisely. Nevertheless, the value of $4 \cdot 10^{-4}$ was assumed to be the maximum activation and corresponding activation thresholds are plotted in Fig. 22. From the available data, the activation thresholds for the sst2 knockout and the samples with no galactose induction are obviously lower than the activation thresholds of wild-type samples and the samples induced with 2% galactose.

5 Discussion

In this work, a mathematical model with derived mechanism for tuning the yeast pheromone pathway activation was introduced. It was mathematically derived that the pathway activation can be tuned by varying levels of the Sst2 protein under certain assumptions. Series of experiments was performed in order to validate the model *in vivo*. For now, data for a wild-type strain, for sst2 knockout and for two different Sst2 levels are available that were measured for three different α-factor concentrations. The experimental data indicate that by varying the Sst2 concentrations the pathway response can be influenced as the model predicts. Nevertheless, more experimental data need to be collected to fully confirm the behaviour predicted by simulations.

Plasmid carrying pFUS1-GFP is being prepared that will allow measuring the pheromone-dependent transcriptional induction instead of measuring only the growth arrest which has shown to be difficult to determine for lower pheromone levels. Also plasmid carrying pSST2-GFP for characterisation of the SST2 native promoter (pSST2) has been assembled that will allow comparing the SST2 levels synthesised from the native SST2 promoter and from the variously induced pGAL1.

References

[1] Jessica Andersson, David M Simpson, Maosong Qi, Yunmei Wang, and Elaine a Elion. Differential input by Ste5 scaffold and Msg5 phosphatase route a MAPK cascade to multiple outcomes. *The EMBO journal*, 23(13):2564–2576, 2004.

[2] Donald M. Apanovitch, Kevin C. Slep, Paul B. Sigler, and Henrik G. Dohlman. Sst2 is a GTPase-activating protein for Gpa1: Purification and characterization of a cognate RGS-Gα protein pair in yeast. *Biochemistry*, 37(14):4815–4822, 1998.

[3] Daniel R. Ballon, Paul L. Flanary, Douglas P. Gladue, James B. Konopka, Henrik G. Dohlman, and Jeremy Thorner. DEP-Domain-Mediated Regulation of GPCR Signaling Responses. *Cell*, 126(6):1079–1093, 2006.

[4] Lee Bardwell. pathway. 26(2):339–350, 2011.

[5] Scott a. Chasse, Paul Flanary, Stephen C. Parnell, Nan Hao, Jiyoung Y. Cha, David P. Siderovski, and Henrik G. Dohlman. Genome-scale analysis reveals Sst2 as the principal regulator of mating pheromone signaling in the yeast Saccharomyces cerevisiae. *Eukaryotic Cell*, 5(2):330–346, 2006.

[6] H G Dohlman, J Song, D Ma, W E Courchesne, and J Thorner. Sst2, a negative regulator of pheromone signaling in the yeast Saccharomyces cerevisiae: expression, localization, and genetic interaction and physical association with Gpa1 (the G-protein alpha subunit). *Molecular and cellular biology*, 16(9):5194–5209, 1996.

[7] Tiffany Runyan Garrison, Yanni Zhang, Mark Pausch, Donald Apanovitch, Ruedi Aebersold, and Henrik G. Dohlman. Feedback phosphorylation of an RGS protein by MAP kinase in yeast. *Journal of Biological Chemistry*, 274(51):36387–36391, 1999.

[8] Nan Hao, Necmettin Yildirim, Yuqi Wang, Timothy C. Elston, and Henrik G. Dohlman. Regulators of G protein signaling and transient activation of signaling: Experimental and computational analysis reveals negative and positive feedback controls on G protein activity. *Journal of Biological Chemistry*, 278(47):46506–46515, 2003.

[9] Bente Kofahl and Edda Klipp. Modelling the dynamics of the yeast pheromone pathway. *Yeast*, 21(10):831–850, 2004.

[10] Saurabh Paliwal, Pablo A Iglesias, Kyle Campbell, Zoe Hilioti, Alex Groisman, and Andre Levchenko. MAPK-mediated bimodal gene expression and adaptive gradient sensing in yeast. *Nature*, 446(7131):46–51, March 2007.

[11] Christopher J Roberts, Bryce Nelson, Matthew J Marton, Roland Stoughton, Michael R Meyer, Holly A Bennett, Yudong D He, Hongyue Dai, Wynn L Walker, Timothy R Hughes, Mike Tyers, Charles Boone, and † Stephen H Friend. Signaling and Circuitry of Multiple MAPK Pathways Revealed by a Matrix of Global Gene Expression Profiles. *Science*, 287(5454):873–880, February 2000.

[12] Adam M Smith, Wen Xu, Yao Sun, James R Faeder, and G Elisabeta Marai. RuleBender: integrated modeling, simulation and visualization for rule-based intracellular biochemistry. *BMC Bioinformatics*, 13(Suppl 8):S3, 2012.

[13] Ryan Suderman and Eric J. Deeds. Machines vs. Ensembles: Effective MAPK Signaling through Heterogeneous Sets of Protein Complexes. *PLoS Computational Biology*, 9(10), 2013.

[14] J Peter Svensson, Laia Pesudo, Rebecca C Fry, Yeyejide a Adeleye, Paul Carmichael, and Leona D Samson. Genomic phenotyping of the essential and non-essential yeast genome detects novel pathways for alkylation resistance. *BMC Systems Biology*, 5(1):157, 2011.

[15] Alan J Whitmarsh. Regulation of gene transcription by mitogen-activated protein kinase signaling pathways. *Biochimica et biophysica acta*, 1773(8):1285–1298, 2007.

[16] Tau-Mu Yi, Hiroaki Kitano, and Melvin I Simon. A quantitative characterization of the yeast heterotrimeric G protein cycle. *Proceedings of the National Academy of Sciences of the United States of America*, 100(19):10764–10769, 2003.

[17] Richard C Yu, C Gustavo Pesce, Alejandro Colman-lerner, Larry Lok, David Pincus, Eduard Serra, Mark Holl, Kirsten Benjamin, Andrew Gordon, and

Roger Brent. Transmission in Yeast Pheromone Response. *Sciences-New York*, 456(7223):755–761, 2009.

A Modelling approaches

A.1 Deterministic approaches

Approaches described in this section were used for construction of a deterministic model of G-protein cycle described in Sec. 3.4 that was further analysed in detail and that introduced an insight into Sst2 behaviour.

Mass action kinetics For the purpose of constructing a deterministic model, a set of chemical reactions can be transformed into a mathematical model using the Law of mass action. Resulting systems of non-linear ordinary differential equations describe how concentrations of reaction species change with time.

Transformation of a simple chemical reaction using Mass action kinetics is shown below. Consider reaction

$$A + B \xrightarrow{k} C \tag{48}$$

corresponding ordinary differential equations, that represent changes in concentration of A, B and C in time are the following:

$$\begin{aligned} \frac{d[C]}{dt} &= k[A][B], \\ \frac{d[A]}{dt} = \frac{d[B]}{dt} &= -k[C], \end{aligned}$$

where k is the reaction rate.

Michaelis-Menten kinetics Michaelis and Menten in fact introduced the idea of time-scale separation into biochemistry. Part of the system is assumed to operate much more faster than the rest so it is considered in equilibrium. They presented a model of enzyme kinetics that relates reaction rate of enzymatic reaction to concentration of a substrate. The reaction is following:

$$E + S \underset{k_r}{\overset{k_f}{\rightleftharpoons}} ES \xrightarrow{k_c} E + P, \tag{49}$$

assuming the concentration of enzyme is much lower that the substrate concentration. k_f, k_r and k_c are reaction rates of enzyme-substrate association, the complex dissociation and catalysed dissociation, respectively. Enzyme enters the

reaction, binds to a substrate to form a complex and leaves reaction in unchanged state while catalysing the reaction. Therefore, total amount of enzyme is assumed to be constant and equal to E_T:

$$[E] + [ES] = [E]_T \tag{50}$$

Equilibrium is expressed by equal rates of forward and reverse reactions:

$$k_f[E][S] = k_r[ES] \tag{51}$$

Combining the assumptions and using Law of mass action (Section A.1) rate of product formation is

$$v_P = \frac{dP}{\mathrm{d}t} = \frac{V_{max}[S]}{K_d + [S]}, \tag{52}$$

where $K_d = \frac{k_r}{k_f}$ is dissociation constant and $V_{max} = k_c[E]_T$ is the maximum rate. When cooperative binding[2] is considered, rate of product formation satisfies

$$v_P = \frac{V_{max}[S]^n}{K_d + [S]^n}. \tag{53}$$

This form is called Hill function where n is Hill coefficient.

Hill function This type of transfer function is frequently used in biochemistry. It describes binding of ligand to a molecule, that is enhanced when there are already other ligands bound to the molecule. Hill function of order n has one of two forms depending on whether the reaction has activation or repression character. The form for a rate of reaction is

$$v_A = \frac{V_{Amax}[S]^n}{K + [S]^n} \text{ for activation, and} \tag{54}$$

$$v_R = \frac{V_{Rmax}}{1 + [S]^n} \text{ for repression.} \tag{55}$$

[2] when one molecule of type E can bind n molecules of type S

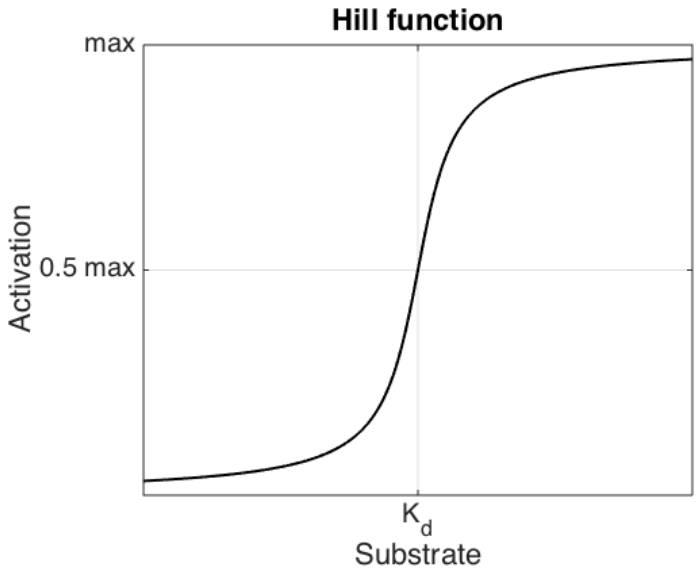

Figure 23: The Hill function behaviour.

A.2 Simulation tools

RuleBender RuleBender is a free tool for modelling and simulating signalling networks in cell [12]. This interface enables writing a script in the BioNetGen language and running it using NFsim simulator.

BioNetGen language uses rule-based approach to describe a model. "BioNetGen input file contains definitions of molecules, reaction rules, chemical and mathematical constants, initial molecule populations, and simulation instructions" [12]. From such an input file, species graph is generated that enables visualisation of protein-protein interaction.

NFsim is also free, open-source simulator of biochemical reactions is fully integrated with BioNetGen. It is efficient even for simulating large and complex networks. Models written in BioNetGen can be simulated both deterministically and stochastically and the results can be compared. Output are the molecule numbers plotted in time. RuleBender was used for stochastic simulations of the complex model mention further.

MATLAB MATLAB and its ODE solver was used for simulations with the simple deterministic model and also the final model with modifications was designed in MATLAB.

B Model parameters

Parameter	Value	Description	Source
k_{Rs}	4 mpc s^{-1}	Synthesis of Ste2	[16]
k_{RL}	$2 \cdot 10^6$ $M^{-1}s^{-1}$	Binding of Ste2 and α-factor	[16]
k_{RLm}	$1 \cdot 10^{-2}$ s^{-1}	Dissociation of Ste2 and L	[16]
k_{Rd0}	$4 \cdot 10^{-4}$ s^{-1}	Degredation of Ste2	[16]
k_{Rd1}	$4 \cdot 10^{-3}$ s^{-1}	Degredation of active Ste2	[16]
k_{Ga}	$1 \cdot 10^{-5}$ $mpc^{-1}s^{-1}$	GDP-GTP exchange rate	[16]
k_{G1}	1 $mpc^{-1}s^{-1}$	Binding of Gα-GDP and G$\beta\gamma$	[16]
k_{Gd0}	$1 \cdot 10^{-3}$ s^{-1}	Basal GTPase rate	[16]
k_{Gd1}	0.11 s^{-1}	Maximal Sst2 activity	[16]
$[Gt]$	$1 \cdot 10^4$	Total number of G-proteins per cell	[16]
$[Sst2]$	$5 \cdot 10^3$	Total number of Sst2 molecules per cell	[8]
$[Ste2]_0$	$1 \cdot 10^4$	Initial number of inactive receptors per cell	[8]
k_H^D	$2 \cdot 10^3$	Hydrolysis dissociation constant	This work
n_H	2	Hydrolysis cooperativity	This work
k_M	$1 \cdot 10^3$ s^{-1}	MAPK maximum rate	This work
k_M^D	$7 \cdot 10^3$	MAPK dissociation constant	This work
n_M	2	MAPK cooperativity	This work

mpc stands for "molecules per cell"